Assessing the Impact of a Railway Tunnel on Groundwater Flow Regime in Urban Areas: A Case Study of Bratislava's TEN-T Track and Proposed Mitigation Measures

Dana Baroková *[ID], Andrej Šoltész [ID] and Michaela Červeňanská

Department of Hydraulic Engineering, Faculty of Civil Engineering, Slovak University of Technology in Bratislava, Radlinského 11, 810 05 Bratislava, Slovakia; andrej.soltesz@stuba.sk (A.Š.); michaela.cervenanska@stuba.sk (M.Č.)
* Correspondence: dana.barokova@stuba.sk; Tel.: +421-902-219-567

Abstract: The Bratislava region in Slovakia aims to improve its transport infrastructure by connecting the airport with the railway network. As part of the Trans-European Network for Transport project (TEN-T), an underground railway line is proposed to be constructed on both sides of the Danube River, connecting the airport in Bratislava to the Petržalka region on the river's right side. However, underground construction is likely to have an impact on the groundwater flow regime. This construction, which will be built below the ground surface, should be built by excavating from above under the protection of sealing walls to prevent significant changes to the groundwater level regime (GWL). Therefore, a numerical model based on the finite element method (FEM) was established to evaluate the effect of the planned underground construction on the GWL, and technical measures were introduced to mitigate any potential impacts. The results of the model revealed possibilities for controlling the groundwater level in the aquifer affected by the railway structure during and after the construction.

Keywords: surface and ground water interaction; finite element method; numerical simulation; technical measures; the Danube River; observation well

1. Introduction

The world population has been increasing at an alarming rate. A majority of this growth is occurring in urban areas [1]. By 2030, urban dwellers are projected to constitute nearly 60% of the global population [2]. The impact of two main constraints, anthropogenic pressure and property economics, has led to the vertical development of urban areas [3]. Underground structures below groundwater level often modify natural groundwater flow, especially in the aquifers of urban regions [4]. This phenomenon was reviewed in [5], which presented the state-of-the-art on the impacts of disturbances caused by underground structures (tunnels, basements of high-rise buildings, deep foundations, etc.) on groundwater flow in urban aquifers.

Several case study examples from all over the world provide proof for previous claims, for example, the subway construction in Barcelona, Spain [6], where the tunnel cut a large section of the Llobregat Delta Shallow Aquifer. Major modifications in the distribution of the groundwater head can be observed when underground structures transversally cut an aquifer, as has been analyzed in Milan and Turin, Italy [7,8]. The same behavior problem was investigated between the construction of the mechanized twin tunnels of the Shiraz metro line and the groundwater [9] in Tehran, Iran. The effect of pre-existing underground structures on groundwater flow induced by dewatering and excavation was examined based on the actual excavation of a metro station in Tianjin, China [10].

According to [11,12], the lack of understanding of the interactions between different structures and groundwater flow remains an obstacle to improving urban planning. In particular, understanding the flow of groundwater in an urban context is the first step in

improving quantitative and qualitative groundwater resources. All the mentioned case studies have one common denominator: they have analyzed the impact of underground structures on groundwater flow under urban conditions using 3D numerical modeling (either the finite element (FEM) or the finite difference method (FDM)). Even with this common denominator, it is quite complicated to compare the results of the analyzed studies due to their different hydrogeological conditions (hydraulic conductivity and thickness of aquifer) and construction processes.

The planned TEN-T track project is part of the Trans-European Network for Transport (TEN-T). Transport networks (roads, railways, airways, and waterways) have been planned or constructed within the TEN-T framework in order to make them usable for all European countries, without any limitations [13].

The first part of the planned project in Bratislava city is the connection between the airport and the railway network. The second part, which is the technically and economically most demanding section of the planned project, will be the design of the alignment of the rail line between the Bratislava Slovany-Bratislava Filiálka and Bratislava Petržalka railway stations (RWS) (red lines in Figure 1). This section should be built in an underground tunnel along the Carpathian Mountains and will significantly affect the groundwater flow regime. This was the reason for creating a quasi-3D finite element numerical model to evaluate the impacts of the railway tunnel on the groundwater level regime, whereby we assumed that this model would serve to simulate the groundwater regime after implementing the technical measures proposed by us [14]. This section of the route passes through a densely developed area of the central urban zone, crosses the Danube riverbed, and connects an existing rail line. Large development projects comprising multi-story buildings are under preparation for a part of the area that is in direct contact with the route. Therefore, the underground route of the rail line is unavoidable. With respect to the sensitive character of the urban area, any negative effect on the surface must be minimized as much as possible or eliminated.

(**a**)

(**b**)

(**c**)
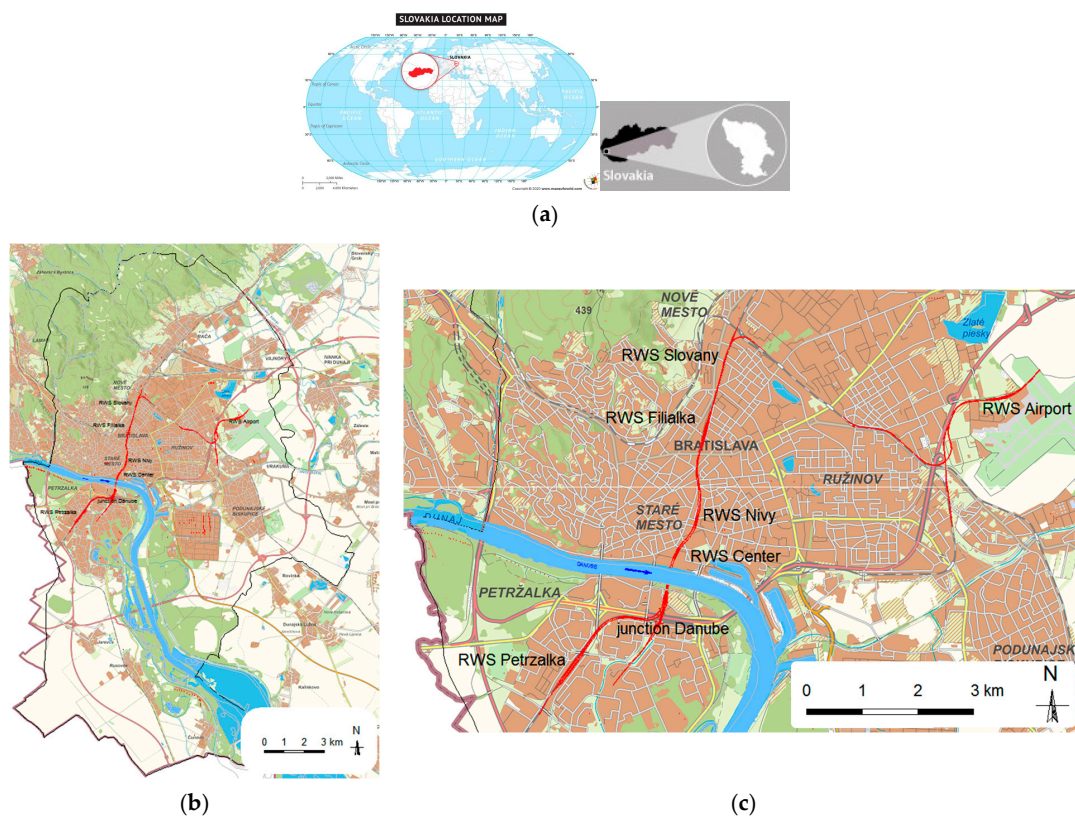
Figure 1. (**a**) Map showing the location of Bratislava in Slovakia [15]. (**b**) General overview of the region under investigation in Bratislava (background map [16]). (**c**) Detail of the surveyed territory [17].

(The red lines indicates the section connecting Bratislava Predmestie-Bratislava and Filiálka-Bratislava Petržalka with the airport of Bratislava, the blue arrow indicates the direction of the Danube flow, red dots indicates GW sources).

The horizontal alignment within this section was affected, above all, by the possibilities of locating stations within the developed area of the city. The vertical alignment is limited by the existing substructures of the so-called Eurovea complex on the left bank of the Danube River, which must be traversed by the route. Since the railway interconnection will also fulfill the function of the urban mass transit system, in addition to the function of the transit, there are two underground stations in the section: RWS Nivy and RWS Center (Figure 2). Another part of the route that is difficult to construct is the Danube junction on the Petržalka side of the river, which is designed to connect the route with the urban mass transit system [13].
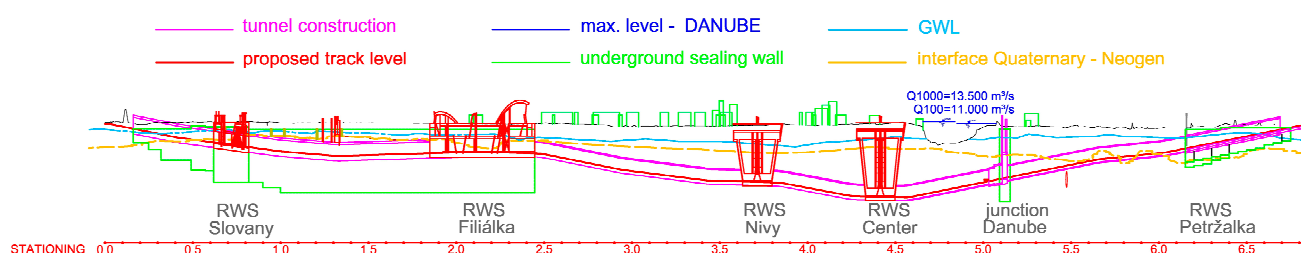
Figure 2. General overview of planned TEN-T track in Bratislava (longitudinal profile) [17,18].

2. Materials and Methods

2.1. Geological, Hydrogeological, and Geomorphological Conditions

The railway link route that is being designed is located in an area that was first formed by the Danube River. The geological structure of the area through which the route passes comprises three types of ground environments: anthropogenic sediments, Quaternary fluvial sediments, and Neogene sediments.

Quaternary fluvial sediments are found on both banks of the Danube River—at a greater distance from the river—in the form of terraces whose thicknesses decrease toward the slopes of the Little Carpathians. They usually consist of gravel and sandy gravel, which contain a variable proportion of sand. Gravel grains are worn by water as their sizes are largely smaller than 30 mm and, less frequently, even larger, up to 100 mm. They consist mainly of hard quartzite, granite, limestone, and crystalline schist. The occurrence of boulders of 300 to 500 mm in diameter in contact with the Neogene bedrock has been recorded in several exploration works. The thicknesses of the layers of Quaternary sediments found along the route ranges from 8 to 14 m. Quaternary sediments are very permeable; therefore, they form a significant corridor for groundwater flows. They are supplied with rainwater, water that flows down the slopes of the Little Carpathians, and, primarily, water that seeps from the Danube River. Therefore, the fluctuations in the water table level follow, with a time delay, the fluctuations in the water surface of the Danube River [17]. Neogene sediments make up the subbase of the Quaternary sediments, and they are represented by cohesive soils and sands with abrupt and irregular alternations in their layers. Soils originate from sedimentation at the edge of a former Palaeogene sea or in the beds of rivers and streams that end in the sea. The main groundwater aquifer is created by fluvial gravel layers and Neogene sands. The groundwater level in these layers is in direct hydraulic dependence on the level of the Danube River, with a corresponding retardation, that is proportional to the distance from the river bed. Neogene clays are impermeable, but positions of Neogene sands are often water-bearing, mainly with a tension horizon, which, after drilling, stabilizes approximately at the level of the free surface in the Quaternary gravels. According to [19] and previous pumping tests [20], it has been determined that the hydraulic conductivity value k in the horizontal direction is approximately $k = 1 \times 10^{-2}$

to 3×10^{-2} m·s^{-1} for Quaternary gravels. In the case of Neogene sands, the hydraulic conductivity value ranges from $k = 3 \times 10^{-4}$ to 1×10^{-6} m·s^{-1}.

Based on the regional geomorphological classification [21], the solved territory belongs to the area of the Danube Lowland, which is drained by the Danube River. At the same time, the Danube is the dominant natural factor involved in the formation of the relief. In addition to the natural factors involved in the formation of the relief, anthropogenic interventions have had the greatest impact on the current landscape (Figure 3).


(a)　　　　　　　　　　　　　　　　　　　　　　　　　　**(b)**
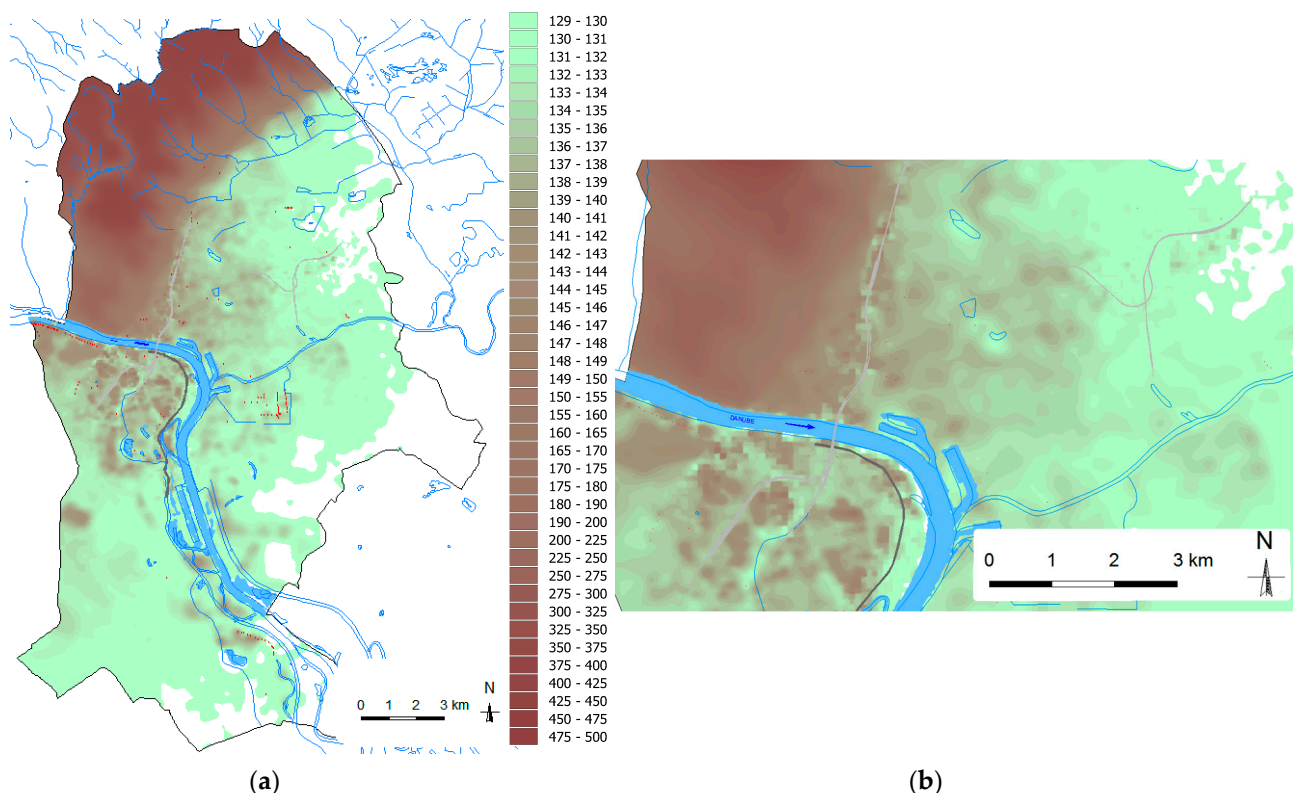
Figure 3. (**a**) Digital terrain model for the construction of the TEN-T. (**b**) Detail of the surveyed territory [17].

2.2. Hydrological Conditions

The hydrological characteristics of the area of interest are clearly determined by the regime of the Danube River, which plays a decisive role as a hydrological factor. In our territory, the Danube River retains the character of a high-mountain (alpine) river. It is fed by alpine snowfields and glaciers, with a typically alpine runoff regime with summer maxima and winter minima. This is caused by the melting of glaciers in the Alps, together with high summer rainfall. Rare high levels in winter can be caused by warm waves that affect snow melting in the lower and middle locations. In the last 40 years, the Danube River has changed its regime due to the construction of a hydropower plant bellow Bratislava. In 1992, the Gabčíkovo power plant (GPP) was put into operation, which caused fundamental changes in groundwater levels in the territory of Petržalka. [22]. After the introduction of the GPP, the flow velocity decreased and the low levels of the Danube River increased by nearly 2 m. In normal operation of the GPP, the level of the Danube River at the 5140 water gauge station in the center of Bratislava should not fall below 131.0 m above sea level. In the last 25 years (1996–2020), the level of the Danube at the gauging station in Bratislava only few times fell below the above-mentioned level, while in the years 2000 and 2001, the level regime had a very similar course, and in 2002, the regime was significantly affected by two flood waves, culminating on 24 March and 15 August 2002. The year 2003 was characterized by a drop in the level, while in the second half of the year, the long-term level was slightly above the elevation level of 131.0 m a.s.l. In 2004 and 2005, the regime

was similar to that before 2002, though with a smaller fluctuation in the water level. The year 2006 was again affected by a flood wave caused by the sudden melting of snow, with a culmination on 2 April 2006. The last recorded flood situation in the Danube River was in June 2013, when the river culminated on 6 June 2013 with a flow rate greater than 10,600 $m^3 \cdot s^{-1}$, according to the Slovak Hydro-meteorological Institute (SHMI) [23]. Part of the course of the river water level in the Danube at Bratislava gauge station 5140 is shown in Figure 4.

(a)

(b)
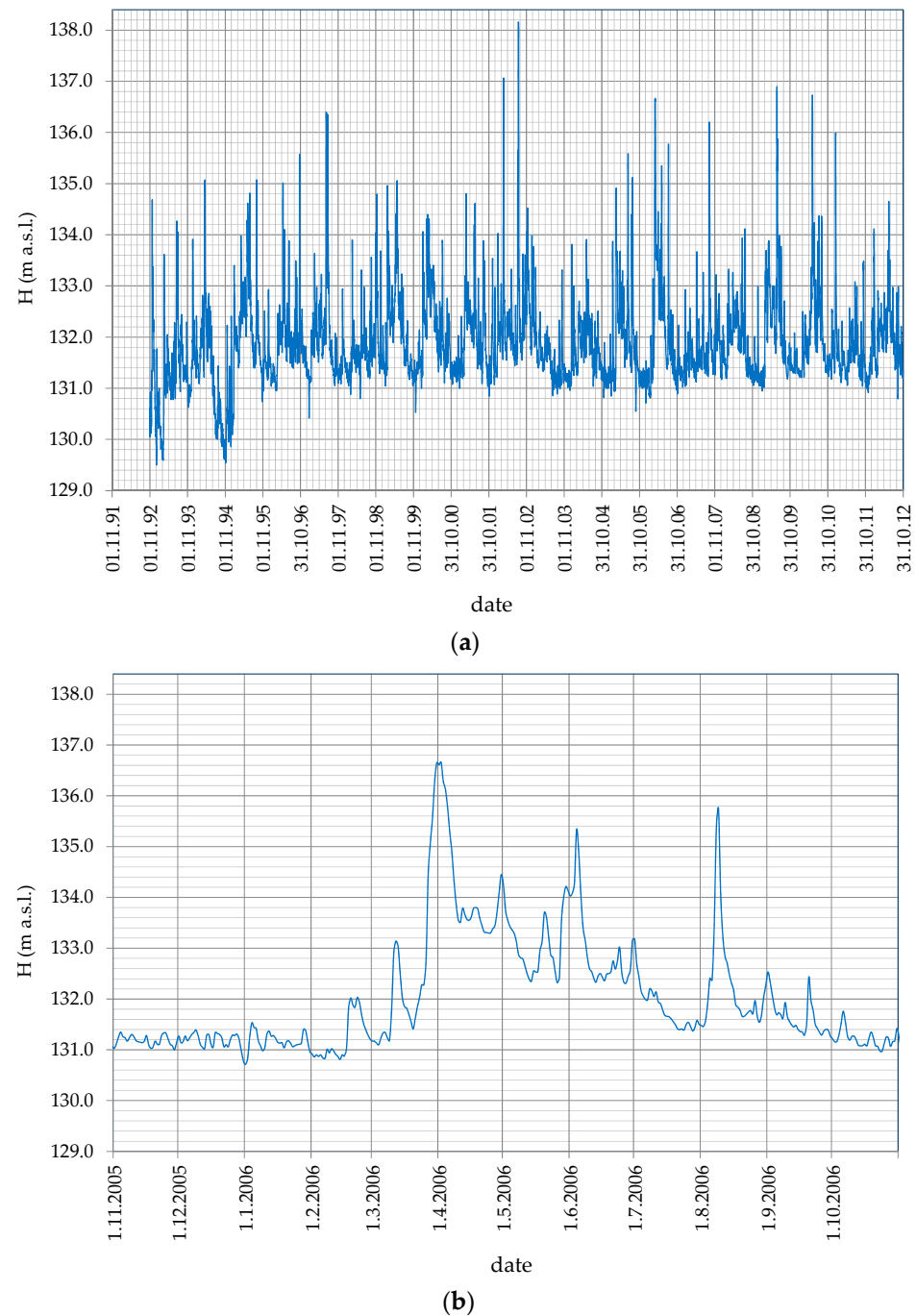
Figure 4. (**a**) The course of the water level in the Danube River at gauge station 5140 Bratislava [23]. (**b**) A zoomed-in view of the hydrological year 2006, which was affected by a flood wave.

In the past, the natural regime of groundwater in the riparian zone was significantly influenced by levels in the Danube up to a distance of 3.0 km from the stream, as evidenced by groundwater level regime measurements taken at SHMI observation wells [24] 7128,

7129, 7130, 7131, and 7121 (Figure 5). The area further away from the Danube had, as it does today, a more stable character, which has also been documented by regime measurements of groundwater levels taken at SHMI observation wells 791, 792, 7167, 7114, 7133, 7166, 7138, and 7125 (Figure 5).


(**a**)　　　　　　　　　　　　　　　　　(**b**)
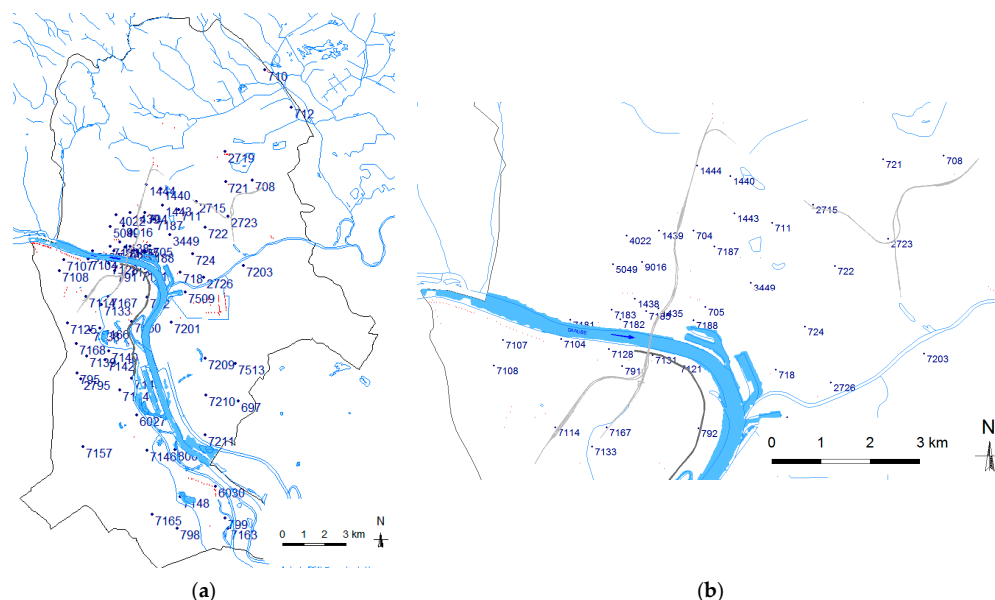
Figure 5. Locations of the SHMI observation wells (**a**) in the Bratislava region, and (**b**) a zoomed-in view of the center of Bratislava and the Petržalka region [17]. (The gray line indicates the section assumed connecting Bratislava Predmestie-Bratislava and Filiálka-Bratislava Petržalka with the airport of Bratislava, the blue arrow indicates the direction of the Danube flow, red dots indicates GW sources.)

2.3. Technical Solution for Protecting the Petržalka Region from Groundwater Flooding

In the 1970s, a hydraulically complete clay-concrete vertical underground sealing barrier was built in the Petržalka region, with a length of 5.5 km (marked in black in Figure 6c), which was embedded 2.5–3.0 m in the Pannonian poorly permeable to impermeable formations [20]. The barrier is located directly within the Danube River flood protection dam, and its purpose is to protect Petržalka against excess surface and groundwater. Recently, a peer-reviewed study on flood risk assessment [25] quantitatively evaluated the risks associated with groundwater during floods induced by surface water flow. The analysis took into account several factors, including the hydraulic regime and the characteristics of the rocks [26] and soil [27].


(**a**)

Figure 6. *Cont.*

(**b**)

(**c**)
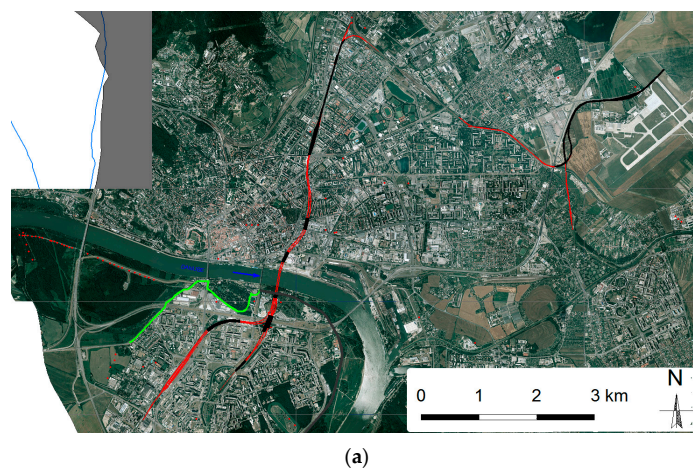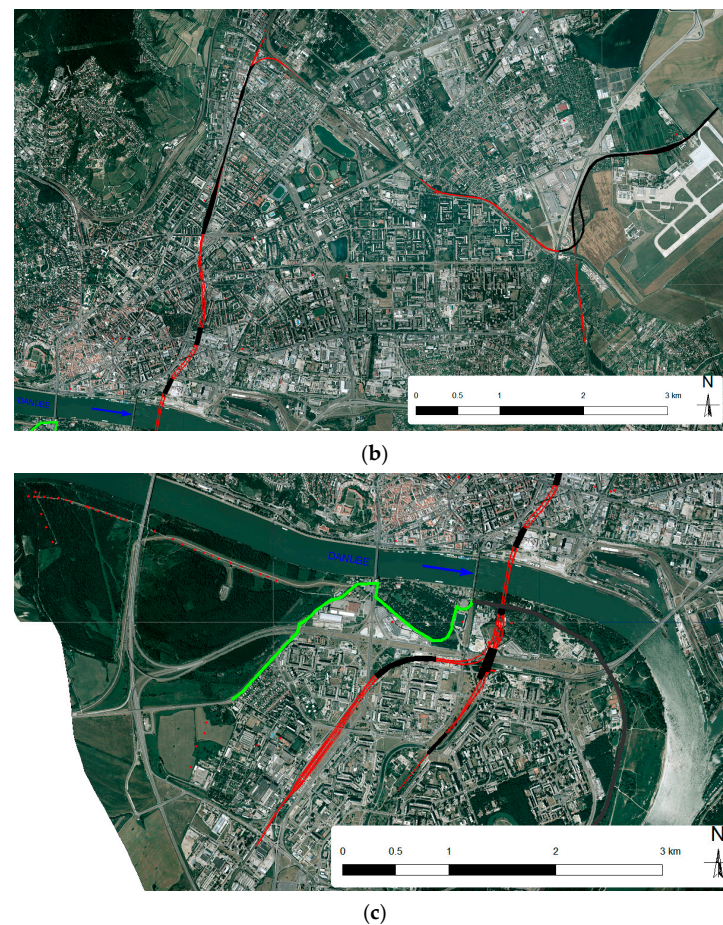
Figure 6. (**a**) Projected track location of the TEN-T connection (highlighted in red) with planed underground sealing walls (highlighted in black) [17] (background [28]). (**b**) A zoomed-in view of the center of the Bratislava region. (**c**) A zoomed-in view of the Petržalka region showing the locations of existing underground sealing walls (highlighted in black) and planned ones (highlighted in green).

Currently, the proposed protection against the seepage of groundwater between the new and old bridges is a hydraulic barrier, which is a system of pumping wells (red dots along the Danube River). There is another underground sealing wall built in this area to protect the residential part of Petržalka against surplus groundwater (marked in black and green, Figure 6) [17]. It should be built perpendicularly to the main direction of the groundwater flow from the Danube River to the residential part of Petržalka. The planned underground railway track for the TEN-T connection is marked in red.

2.4. Design and Assembly of the Conceptual Model

To compile a numerical model of the groundwater flow in the Petržalka area, we extended the original boundary. Figure 7 shows the modified boundary for the filtration area, which was laid out to describe the main characteristics of the natural flow of groundwater in this area and, at the same time, so that the wrong choice for the value of the boundary condition would not have a significant impact on the solution to the problem itself. Depending on the type of boundary condition, two parts could be defined. The blue part expressed the boundary of the area on which the Dirichlet boundary condition (2) was entered (the groundwater level). The red part expressed the edge of the filtering area on which we entered the Neumann boundary condition, i.e., the inflow to the area (3). We entered the groundwater level at the boundary of the filtration area as the average level from the regime measurements in SHMI observation wells. We assumed that the inflow

from the Carpathian side would be zero since the western border could be considered a division line point in the given territory.
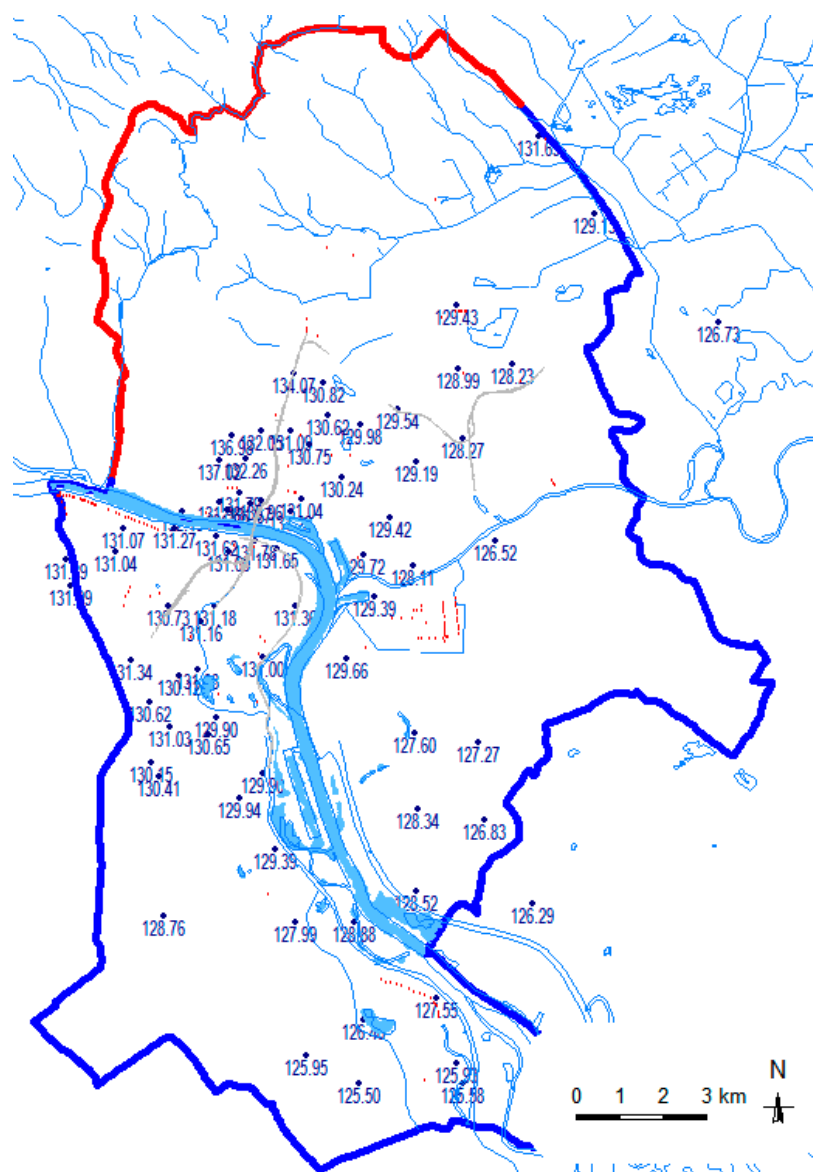
Figure 7. Area of interest with the considered boundaries and indications of the average groundwater levels (m a.s.l.) at the SHMI boreholes. (blue part expressed the Dirichlet boundary condition the red part expressed the Neumann boundary).

To calibrate the model, the level in the SHMI probes was determined as the average for the years 1995–2020, and we performed a verification for the maximum state that occurred in April 2006.

According to projection documentation, all sections of the TEN-T railway track in Petržalka should be built by excavating from above under the protection of retaining and sealing walls. This variant of implementation proved to be the most unfavorable method in terms of its impact on the groundwater level regime.

2.5. Modeling Process

The engineering-geological survey results, derived from available geological documents [19] and augmented with field drilling and survey data gathered for the TEN-T project, in conjunction with supplementary information from the SHMI database, were utilized to perform parameterization of the filtration area.

Parametrization of the individual input values meant assigning the investigated parameter to each node of the finite element simulation network. The aforementioned transformation of spatially orientated data could be performed in several ways. In our case study, we tried three different methods that could be recommended for processing input parameters: the TinInt, InvDist, and Kriging methods [29].

The evaluated background materials were used to create a digital terrain model (Figure 3), a hydraulic conductivity map (Figure 8), a cover layer thickness map, and an aquifer thickness map or a Quaternary-Neogene base interface map (Figure 9). These parameters entered the model as important input values to solve the groundwater level regime.
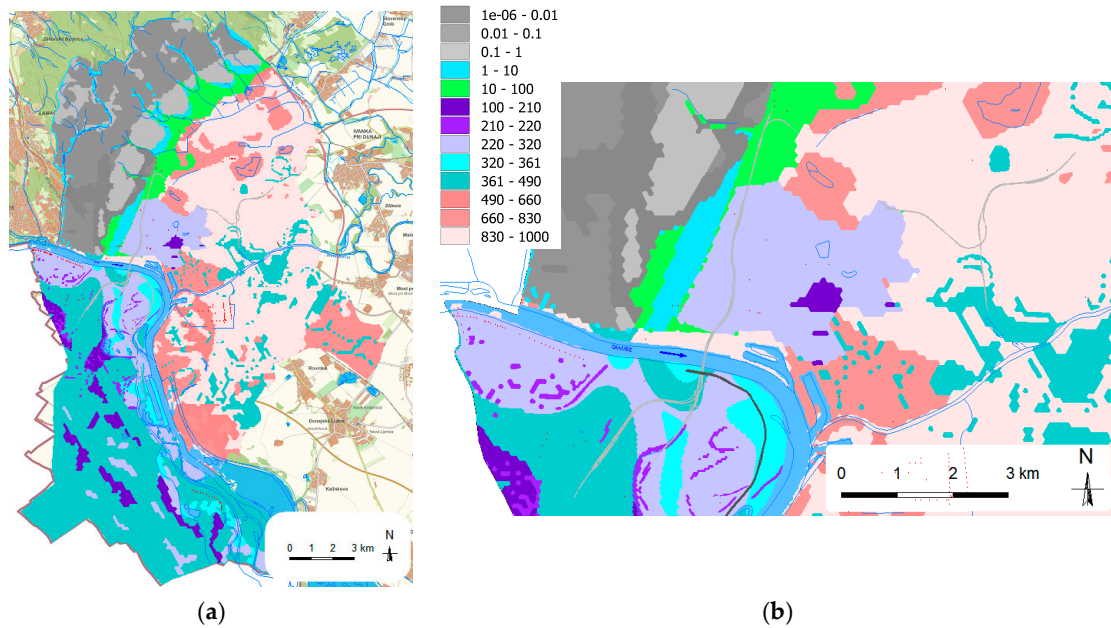
Figure 8. Map of the hydraulic conductivity values (m·d^{-1}) (**a**) in the Bratislava region and (**b**) (zoomed-in) in the center of the Bratislava and the Petržalka region [17].
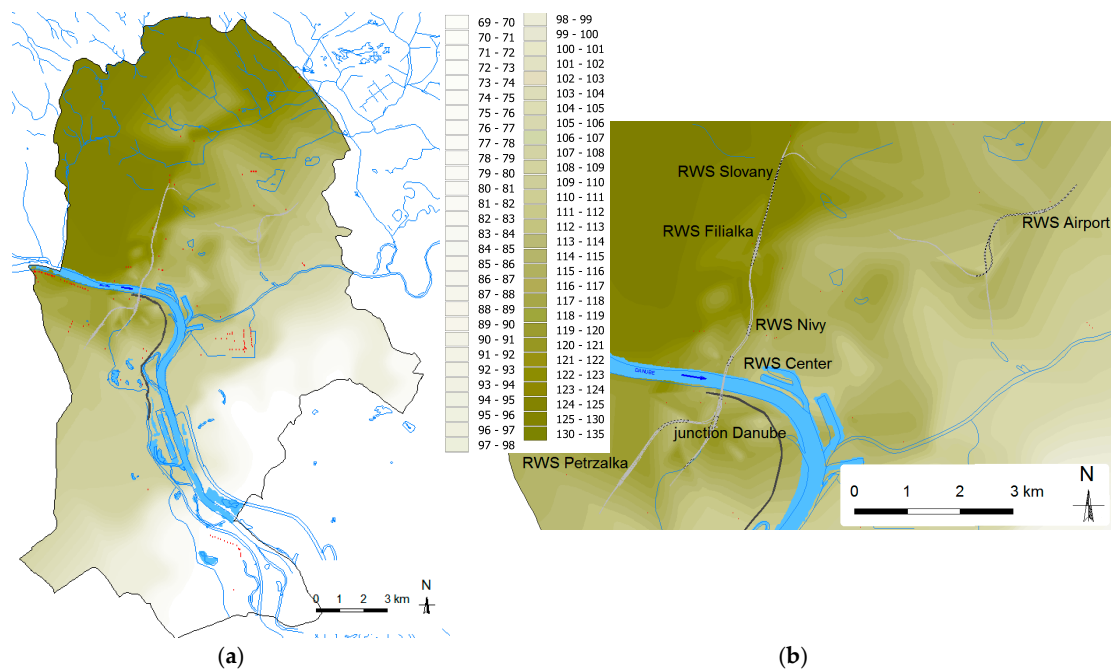
Figure 9. Map of the interface between the base of the Quaternary and Neogene layers (m a.s.l.) (**a**) in the Bratislava region and (**b**) (zoomed-in) in the center of Bratislava and the Petržalka region [17].

From the evaluation of the geological conditions of the territory, it followed that the thickness of the aquifer increased in the direction from west-northwest to east and from a value of 10–18 m to 50–100 m in the south of the territory. The cover layers of soil throughout the territory were mainly created by clay, the thickness of which is relatively low, ranging from 0.5 to 1.2 m and, occasionally, up to 4 m. The hydraulic conductivity values in the area of the future TEN-T railway track range from 100 to 1000 m·d^{-1} (1×10^{-3}–1×10^{-2} m·s^{-1}). According to these values, the aquifer horizon could be evaluated as a rock environment, with very high permeability.

To simulate the groundwater flow, TRIWACO [29] was used. TRIWACO is a simulation software system for the quasi-three-dimensional simulation of continuous groundwater flow based on the finite element method (FEM). The general equation for porous media—partial differential Equation (1) that was solved (by approximation) in the program TRIWACO Flairs—followed from Darcy's law and the equation of continuity. In the derivation of the equation, the Dupuit-Forchheimer assumption was used so that the partial differential equation could be written in terms of the potential 'h' (or groundwater head), as follows:

$$\frac{\partial}{\partial x}\left[T\frac{\partial h}{\partial x}\right] + \frac{\partial}{\partial y}\left[T\frac{\partial h}{\partial y}\right] + q = S\frac{\partial h}{\partial t},$$ (1)

where T is the transmissivity (m^2·s^{-1}), h refers to the piezometric (groundwater) head (m a.s.l), S refers to the storativity (-), and q refers to the recharge (m^3·s^{-1}/m^2).

For a multi-aquifer system, Equation (1) holds for each aquifer, and the top aquifer may be phreatic. The aquifers are coupled through the recharge q, where the components of the recharge are recharged into the aquifers due to precipitation and infiltration from rivers and from point sources due to leakage between aquifers.

In this case, transmissivity is a function of the groundwater head and the hydraulic conductivity of the aquifer, which can spatially vary, while the storativity S changes if the aquifer changes from a confined to a phreatic condition [29].

It is possible to approximate the 3D flow to a quasi-3D flow by dividing the aquifer into several aquifers, and the program uses FEM to carry out a simulation of the groundwater flow or the head (for a quasi-three-dimensional modelling system).

The boundary, necessary to delimit the model, was specified as the boundary of the Bratislava self-governing region. For most of the boundary, the Dirichlet (Type 1) BC was specified as follows:

$$h = h_0(x, y),$$ (2)

where the constant boundary head h_0, based on the long-term monitoring of the groundwater level in the SHMI boreholes, was applied. The area northwest of the boundary in the presented model was formed by the Carpathian Mountains, where the Neumann (Type 2) BC was used to establish the boundaries of the model as follows:

$$k\frac{\partial h}{\partial x}n_x + k\frac{\partial h}{\partial y}n_y = q_0(x, y),$$ (3)

where the constant boundary flux, independent of the groundwater head q_0, is given. In the model, a no-flow boundary was created ($q_0(x, y) = 0$).

Part of the border the Danube River forms in the southeast of the area, and at this border, the Robin (or Cauchy [30]) (Type 3) BC was entered as follows:

$$k_x\frac{\partial h}{\partial x}n_x + k_y\frac{\partial h}{\partial y}n_y = \frac{(h - h_0)}{C}.$$ (4)

In addition, the Danube River, which has a substantial impact on the groundwater level in the area of the study, flows as an internal boundary in the model (the line inside the solved area) on which the internal Robin (Type 3) BC was entered (applied). This meant that if the Danube river water level was HR, a specific flux into or from the simulated area

could be governed by equation $q_r = \frac{(h_r - h)}{C}$, where $C = \frac{b_0}{k_0}$ is the infiltration or drainage resistance (the program offers the possibility to define a different resistance for drainage and for infiltration).

During the actual modeling of the introduction of the underground sealing wall defined in [17,20], the sizes of the elements were gradually refined in order to describe the character of the wall as best as possible. An example of the construction and gradual refinement of the proposed finite element network is shown in Figure 10. The network was made up of elements ranging in size from 2 to 150 m (Figure 10). The generated output grid consisted of 131,103 nodes, 261,074 elements, 151 sources (red dots), and 23 rivers.

When calibrating the model, the groundwater level measurements were required to be compared with the simulated values. We calibrated the model for both the long-term average for the period 1995–2020 (hereafter referred to as the average GWL) and for the maximum GWL that occurred in the given area in April 2006 (hereafter referred to as the maximum GWL).

There was a great dispersion of groundwater levels between the maximum and minimum, which occurred from 1993 to the present. These values showed that the GWL regime in this area is significantly dependent on the level of the Danube River, especially in its coastal part. The depth of the groundwater level varies from 2.83 to 5.88 m below the surface of the terrain.
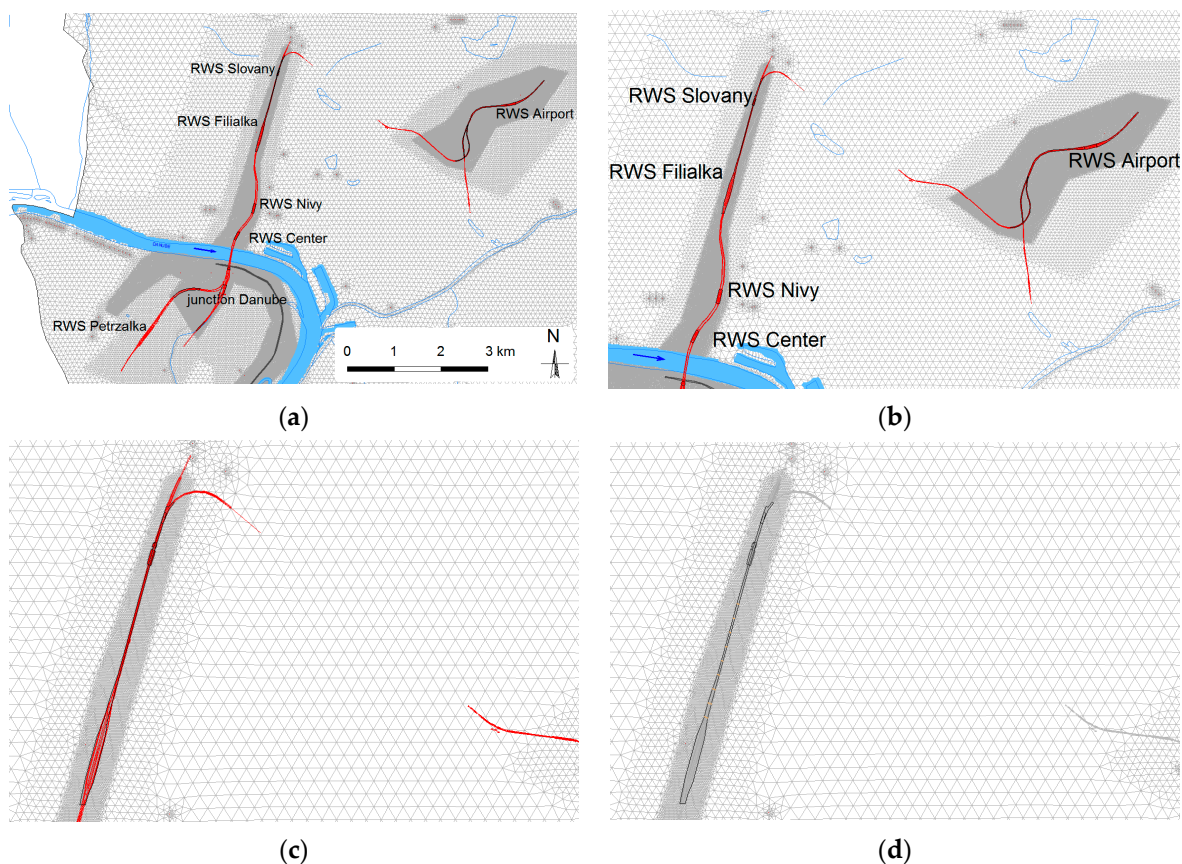

(a)

(b)

(c)

(d)

Figure 10. *Cont.*

(**e**)

(**f**)

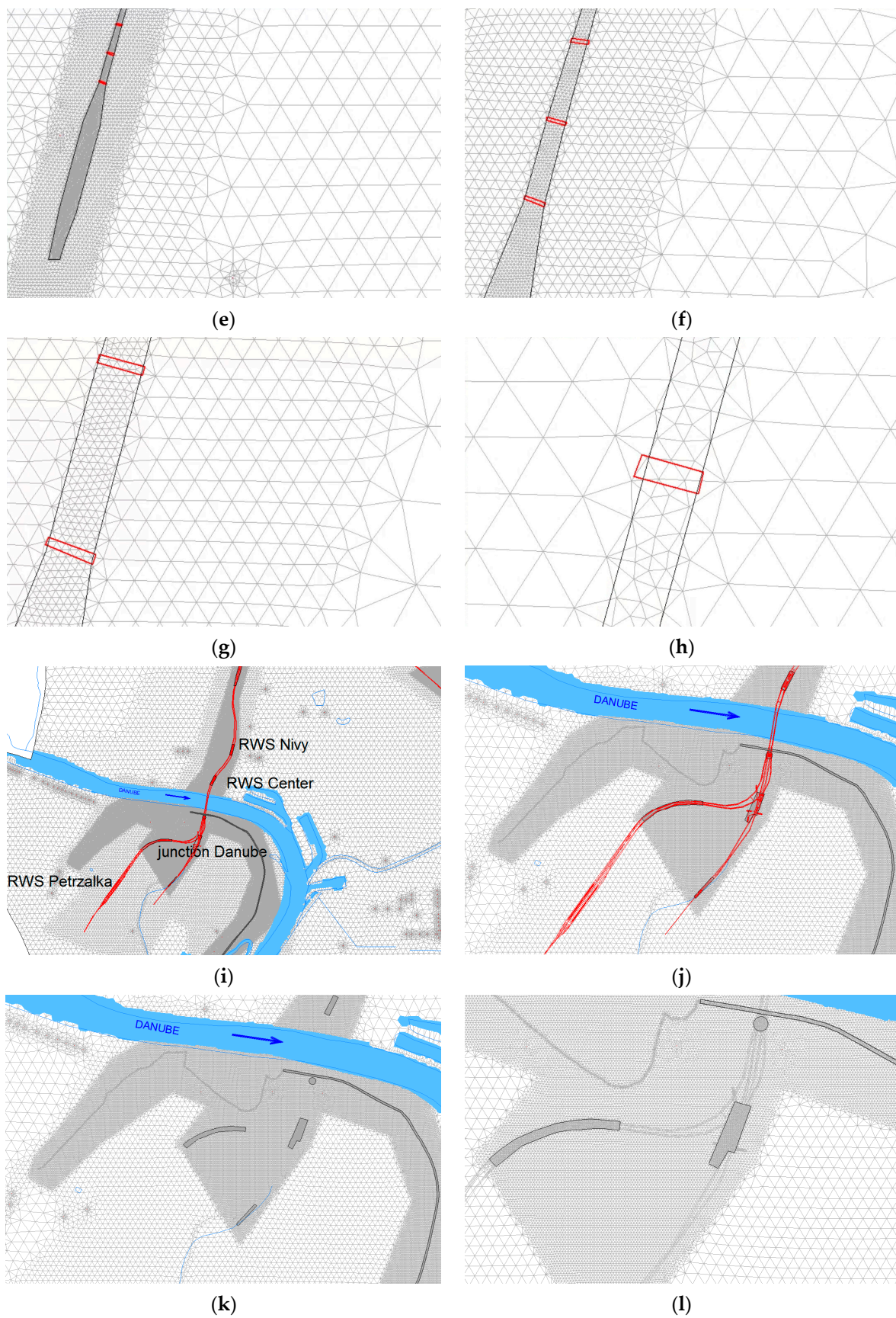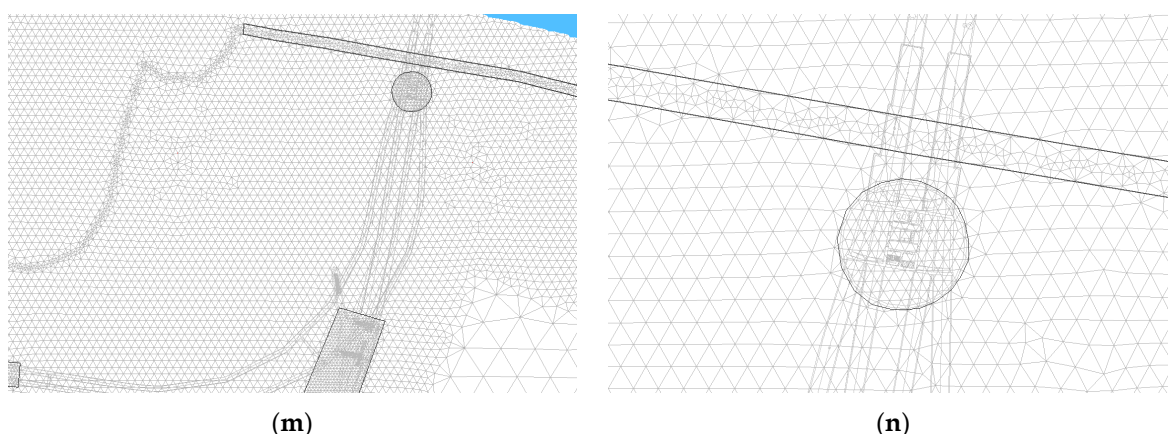(**g**)

(**h**)

(**i**)

(**j**)

(**k**)

(**l**)

Figure 10. *Cont.*

Figure 10. Demonstration of the gradual refinement of the finite element mesh (maximum element length of 150 m and minimum element length of 2 m) (**a**–**h**) in the center of Bratislava and (**i**–**n**) in the Petržalka region [17]. ((**e**,**f**) openings are indicated by a red rectangle).

3. Results

### 3.1. Modeling Results Calibration Process

The mathematical modeling itself using FEM was first performed for the purpose of calibrating the compiled model for the average values of the GWL for the hydrological years 1995–2020, and then verification of the model was performed for the maximum level of GWL corresponding to the month of April 2006.

The calibration of the model consisted of setting the hydraulic and hydrogeological parameters of the aquifer with a detailed view of the area of the future TEN-T route. The calibration parameters were the drainage and infiltration resistance values of the bottom of the streams and the inflow from the slopes of the Little Carpathians in the west and northwest of the area. Another calibration factor was the choice of the interpolation method in the parameterization of the environment. For the parameterization of the input data, the TinInt method appeared to be the most suitable. The selected parameterization results are shown in Figures 8 and 9.
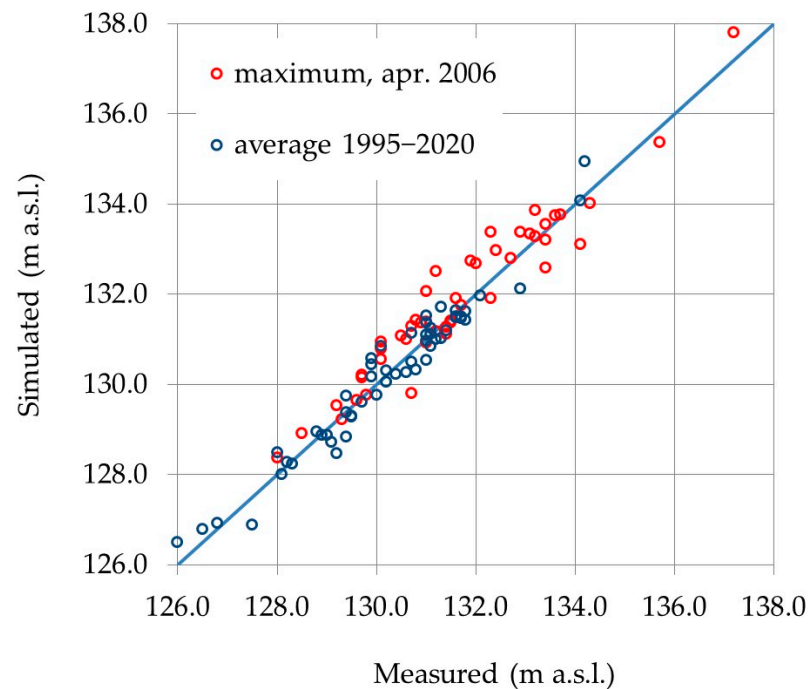
The results of the calibration, i.e., the determination of differences between the measured and simulated GWL values in the monitored area (deviation), are presented in graphic form, as these values are only informative. For the average GWL, they are shown in Figure 11 and for both the average and maximum GWL in Figure 12. The color differentiation of the numbers outlined in the figures indicates positive or negative differences between the measured and simulated values. A positive value (blue) meant that the simulated value was greater than the measured value, and correspondingly, if the value was negative (red), then the simulated groundwater level was lower than the measured value. It can be seen from the images that there are, of course, differences in the average GWL status, and the differences near the area of interest are, at most, up to ±0.70 m. These differences were not negligible, but we believed that even considering the variance in the GWL from 1.33 to 6.33 m, these values were acceptable, which was also confirmed by other calibration criteria, the results of which are shown in the Table 1. Further refinement of the results could be achieved by choosing a different model, as discussed in [31]. However, this was not the primary objective of our research.

Table 1. Comparison of the simulation results for the cluster near the planned TEN-T track project.

Model	Average GWL	Maximum GWL
Minimum deviation (m)	−0.86	−0.95
Maximum deviation (m)	+0.72	+0.83
RMSE (m)	0.127	0.288
NRMS (%)	1.46	3.13

(**a**)

(**b**)
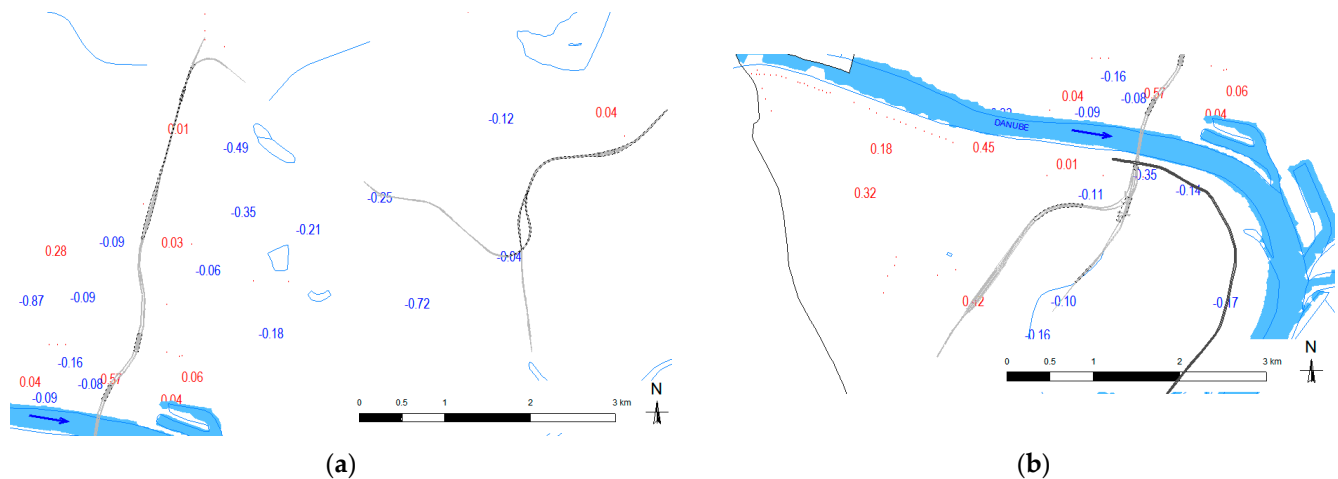
Figure 11. Comparison of the simulation results. The difference (m) between the simulated and measured GWL values (average for the period 1995–2020) in (**a**) the center of Bratislava and (**b**) the Petržalka region [17].

Figure 12. Comparison of the simulated and measured GWL values (average values for the period 1995–2020 and the maximum values from April 2006) [17].

The results of the calibration, i.e., the determination of differences between the measured and simulated can also be compared with the calibration criteria i.e., the quantitative comparative criteria for determining the quality of the model, were determined by the Root Mean Squared Error (*RMSE*) [32] calculation, as follows:

$$RMSE = \left[\frac{1}{n} \sum_{i=1}^{n} (h_m - h_s)_i^2 \right]^{0.5}, \tag{5}$$

where n is the number of checkpoints (observation wells), h_m is the measured GWL (m a.s.l) value at a certain control point i, and h_s is the simulated GWL (m a.s.l) value at the same location.

Another method for determining the calibration criteria (except for the deviation (difference in Figure 11) and *RMSE*) could be the Normalized Root Mean Squared (*NRMS*)

method, which can be normalized according to [33] by the mean (average), the difference between maximum and minimum, the standard deviation, and the interquartile range of the observations. According to [34], a more representative measure of the fit than of the standard *RMSE* is equal to the *NRMS* normalized by the maximum difference in the observed head values (measured GWL), and it is expressed as a percentage and calculated by Equation (6) as follows:

$$NRMS = \frac{RMSE}{h_{m,\max} - h_{m,\min}} \cdot 100 \text{ \%},\tag{6}$$

where $h_{m,\min}$ and $h_{m,\max}$ are the minimum and maximum values, respectively, of the measured GWL.

The calibration results obtained by applying the calibration criteria defined in Equations (5) and (6) are presented in the Table 1.

The final map of GWL isolines for the calibration period for the average GWL status is shown in Figure 13, and the maximum GWL status (April 2006) is shown in Figure 14.
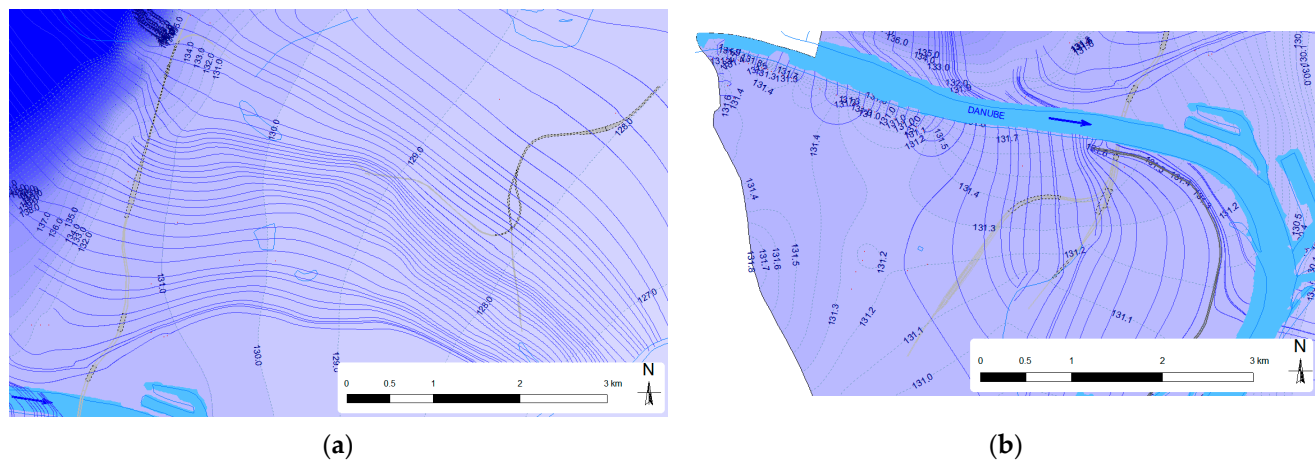
The direction of groundwater flow, as well as the slope of the groundwater level, will slightly affect the slope of the terrain and impermeable subsoil. Based on the model, the direction of groundwater flow was determined (Figure 15). As can be seen, the general direction of groundwater flow was from the northwest to the southeast, that is, from the Carpathian Mountains to the Little Danube, and this is shown in Figure 15a. In Figure 15b, the general direction of the groundwater flow from the Danube River to the south toward the Croatian branch (marked in blue) can be seen. In the east, behind the sealing wall (marked in black), the water does not reach the center of Petržalka, but rather, it flows along this wall.
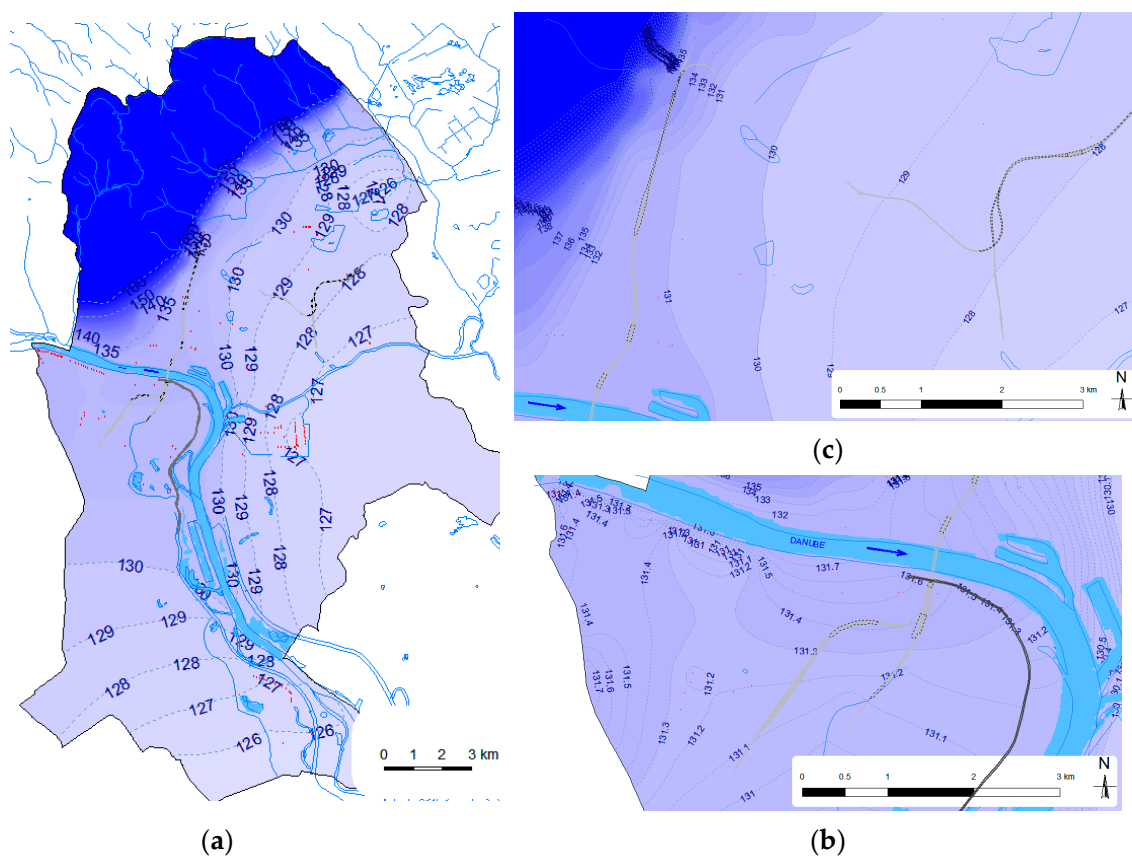
Figure 13. Course of the simulated GWL isolines (m a.s.l.) for the average GWL state (for the period 1995–2020): (**a**) the entire Bratislava region and zoomed-in views of (**b**) the center of Bratislava and (**c**) the Petržalka region [17].

(**a**)   (**b**)

Figure 14. Course of simulated GWL isolines (m a.s.l.) for the maximum GWL state (for the month of April 2006): zoomed-in views of (**a**) the center of Bratislava and (**b**) the Petržalka region [17].

(**a**)   (**b**)

Figure 15. Course of simulated GWL isolines (m a.s.l.) with a simulated direction of groundwater flow for the average GWL state (for the period 1995–2020): zoomed-in views of (**a**) the center of Bratislava and (**b**) the Petržalka region [17].

3.2. Modeling Results Prognosis

After calibration (for the average GWL values) and verification of the model (for the maximum GWL situation for April 2006), we were able to proceed to the next simulation. Due to the fact that the TEN-T connection route will be built in certain sections in a sealed construction pit, it was necessary to design another variant of the model to simulate impermeable construction pits (specified in the TEN-T project documentation [18]). The locations of the mentioned construction pits in the model are evident in Figure 16. These sealed pits are highlighted in black.

Since the TRIWACO simulation software system only considers groundwater flow through a porous medium, we designed the impermeable pits to have a very low hydraulic conductivity value (in the order of hundreds to thousands of m/day) at the location for each future sealed pit.

The result of the simulation with the designed sealed pits (for the average condition) is evident from the floor plan in Figure 17. However, this figure does not have much informative value, and therefore, we preferred to present the direction of groundwater flow with a future sealed pit, as shown in Figure 18, and the difference in GWL, as shown in Figure 19.
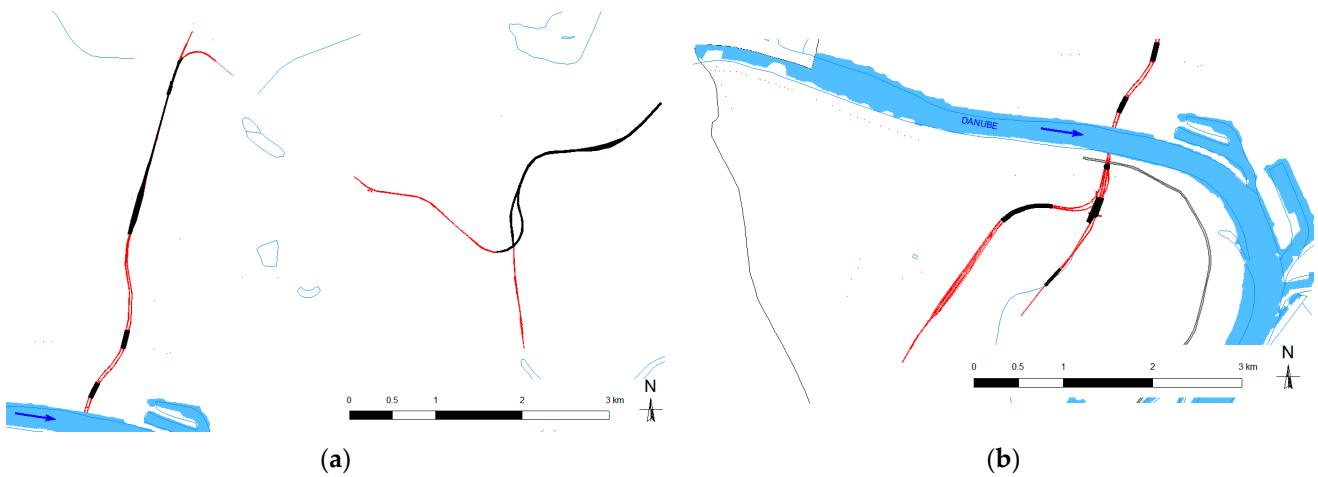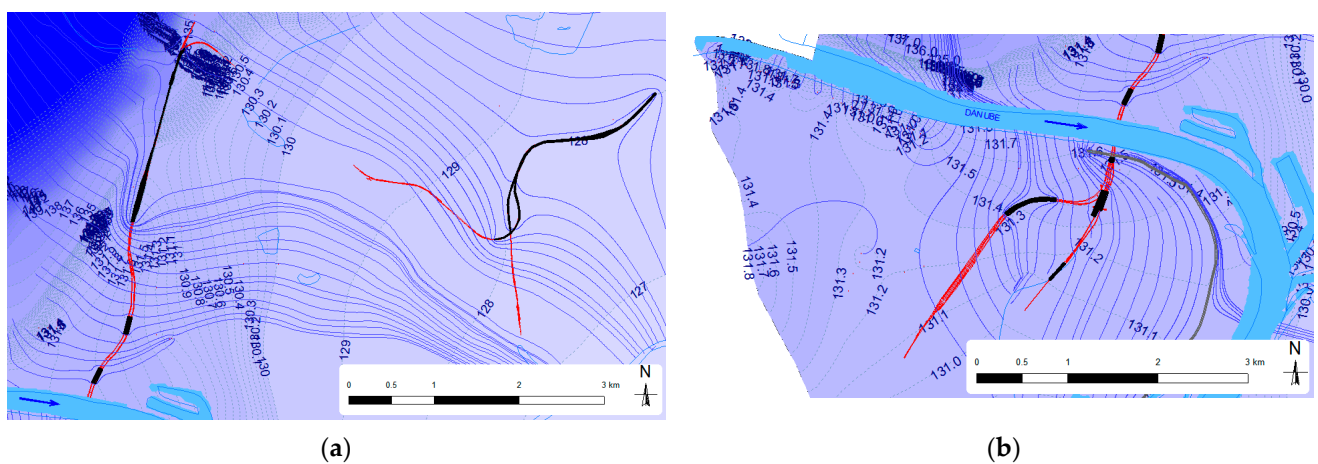
Figure 16. Short sections of the impermeable construction pits along the proposed railway route (black): zoomed-in views of (**a**) the center of Bratislava and (**b**) the Petržalka region.
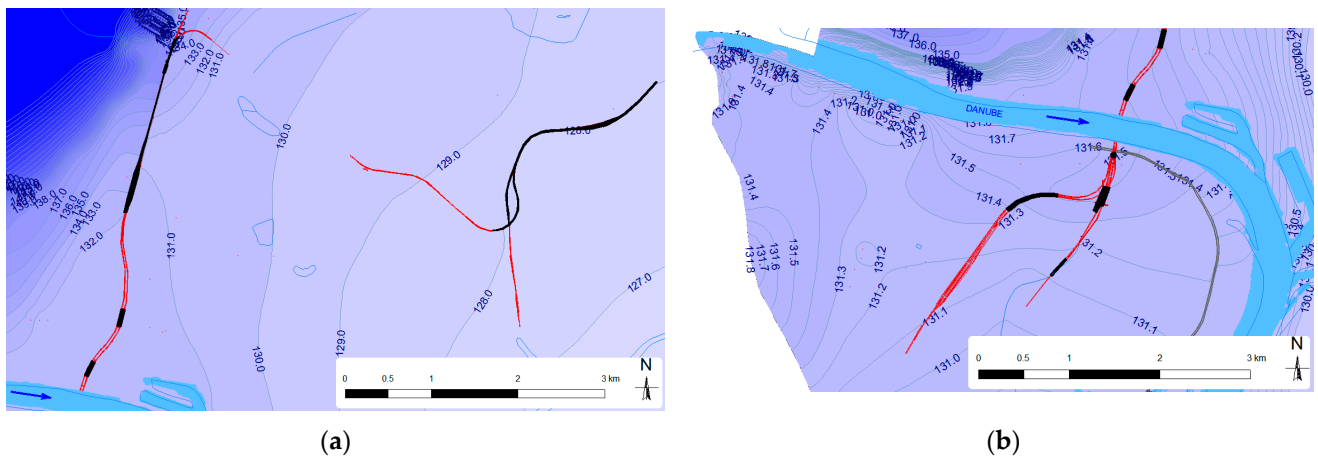
Figure 17. The simulated course of GWL, assuming the construction of short sections of the impermeable construction pits (referred to the average condition): zoomed-in views of (**a**) the center of Bratislava and (**b**) the Petržalka region.
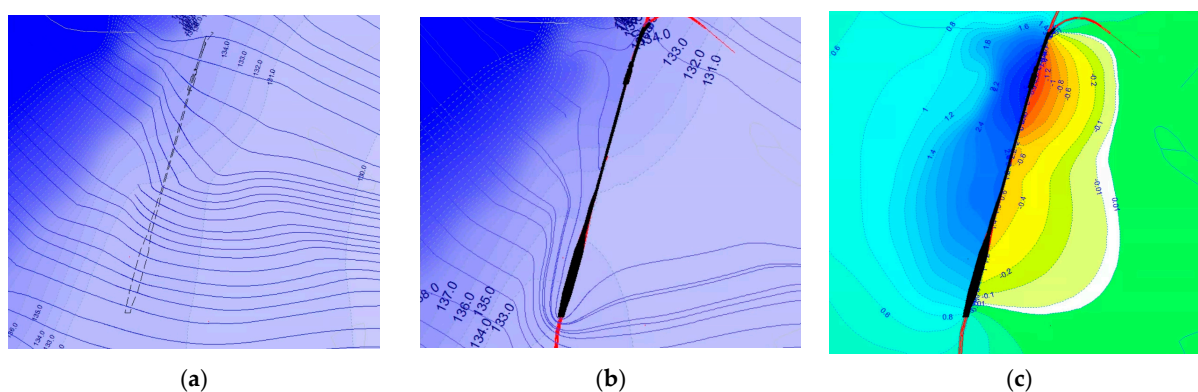

Figure 18. Simulated course of GWL with a simulated direction of groundwater flow, assuming the construction of short sections of the impermeable construction pits (referred to the average condition): zoomed-in views of (**a**) the center of Bratislava and (**b**) the Petržalka region [17].
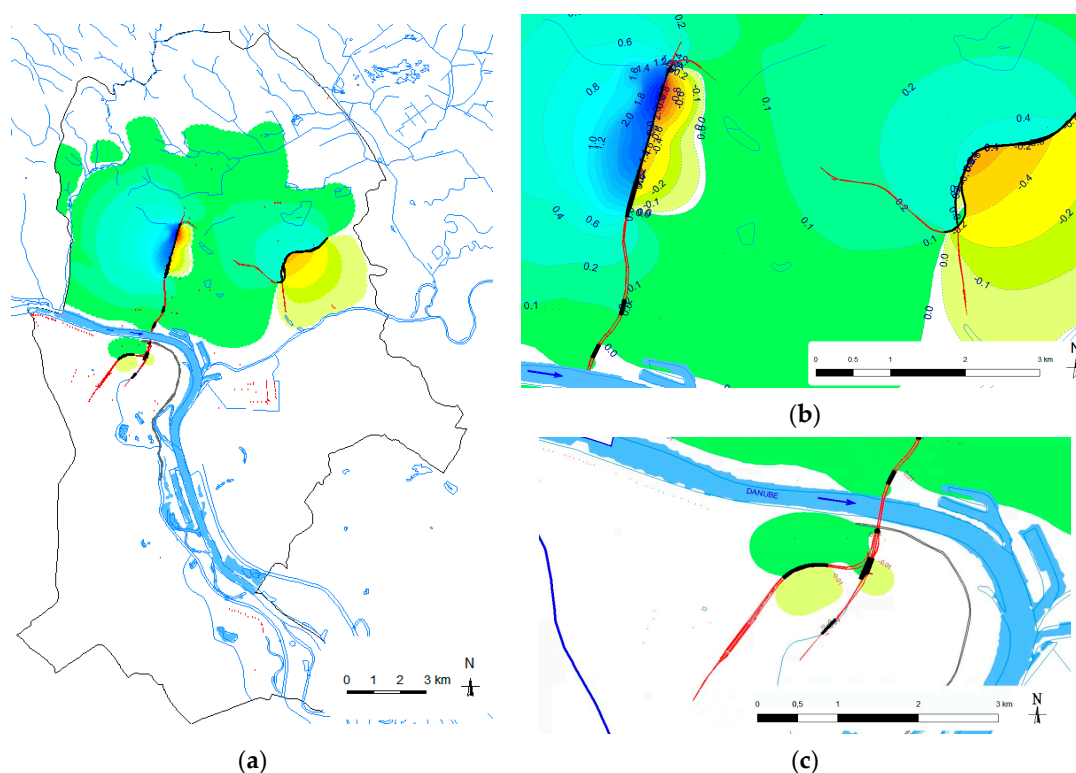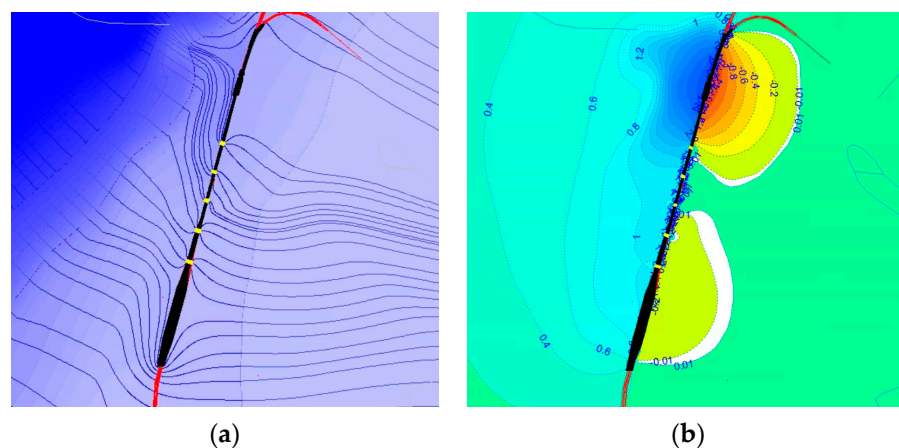
Figure 19. Simulated course of the GWL difference, assuming the construction of the impermeable construction pits (referred to the average condition): (**a**) solution for the entire area, and zoomed-in views of (**b**) the center of Bratislava and (**c**) the Petržalka region.

As can be seen in the previous figures, the construction of underground mined station sections in the Petržalka region and the sealing walls at the airport in Bratislava had no significant impacts. However, in the section of the underground railway track designed to sink from the surface under the protection of the bracing structures, which will at the same time provide protection against the seepage of groundwater into the railway tunnel [13], i.e., in the RWS Slovany–RWS Filiálka section, there could be an increase in groundwater level in some sections by up to 2.5 and even up to 3.5 m from the northwest. Conversely, there could also be a decrease in the groundwater level by 1.5 to 2.5 m from the northeast. Therefore, the research that followed focused specifically on this section, which is shown in more detail in Figure 20.
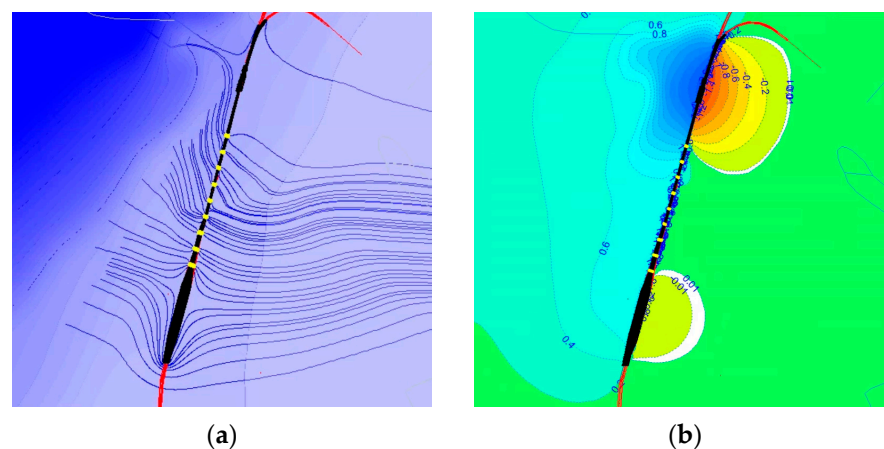

Figure 20. (**a**) Simulated groundwater flow direction with GWL course—natural state; (**b**) simulated groundwater flow direction with GWL course, assuming the construction of the impermeable construction pits; and (**c**) simulated course of the GWL difference. Detailed view in the section RWS Slovany–RWS Filiálka.

In our modeling, we selected an alternative proposal that included the construction of five or nine openings in the sealed wall above the proposed cut-and-cover tunnel of the railway track, where it would be possible for excess water to flow through from the northwest to the northeast. In the groundwater model, these openings were treated as elements with very high values of hydraulic conductivity. The results of the model after implementing these measures are illustrated in Figures 21 and 22.

| (**a**) | (**b**) |

Figure 21. (**a**) Simulated groundwater flow direction with GWL course, assuming the construction of the impermeable construction pits with five openings in the sealed wall, and (**b**) simulated course of the GWL difference. Detailed view in the section RWS Slovany–RWS Filiálka.

| (**a**) | (**b**) |

Figure 22. (**a**) Simulated direction of groundwater flow direction with GWL course, assuming the construction of the impermeable construction pits with nine openings in the sealed wall, and (**b**) simulated course of the GWL difference. Detailed view in the section RWS Slovany–RWS Filiálka.

Based on an analysis of Figures 21 and 22, it was evident that the issue of increased groundwater levels had been significantly mitigated. However, in the specific section of the RWS Slovany, where the implementation of the proposed openings is unfeasible, the problem of high groundwater levels remains unresolved. One possible solution would be to propose the implementation of a drainage element in the northwest of the RWS Slovany, along with an infiltration element in the northeast of the RWS aimed at effectively managing the groundwater level in the area. Simulation of such measures will be the subject of further research.

4. Discussion

The submitted contribution describes a model solution for assessing the planned construction of the TEN-T railway connection between the airport on the left side of the Danube River through the city center on the other side of the Danube to the Petržalka

region, near the area discussed in [35]. There are several sections of this connection which should be built in an underground tunnel along the Carpathian Mountain, as well as under the Danube River.

Due to the fact that the construction route is carried out primarily in the aquifer layer of the rock environment under the Little Carpathians, a numerical model of groundwater flow was compiled using FEM, with the help of which we determined the impact of this construction on the development of the groundwater level regime in the given area, taking into account the influence of the effective precipitation listed in [36].

The solution showed different results for the impacts to the groundwater level regime. On the left side of the Danube River after tunnel construction, above the rail corridor route, there will be an increase in GWL of 1.5–2.0 m for the average or maximum condition (Figure 20). Backwater can be eliminated by designing "openings" in the sealing wall, which we propose to be located in places where it is feasible or as implemented by the model [17]. The designed openings will allow groundwater to flow across the proposed railway track. The solution was performed in two variants, i.e., five openings 180 m apart or nine openings 100 m apart. The decrease in the groundwater level is shown in Figures 21 and 22. The difference between these two variants was not significant, but building more holes speaks in favor of safety. The results of the modeling showed that this proposal would reduce the water level by 1.3–1.6 m compared to the sealing wall without any measures. The groundwater level will be 5.7 to 6 m below the surface, which is an acceptable state, in our opinion [17].

Completely different results were obtained on the right side of the Danube River in the Petržalka region (Figure 19c). The analysis revealed that the construction of the tunnel would cause a minimal and localized increase in groundwater level by only a few centimeters. This finding remained consistent whether considering the average or maximum hydrological conditions. As a result, no remedial measures are necessary to regulate the the groundwater level during the construction of the TEN-T connection.

5. Conclusions

Based on the results of the model solution presented in this paper, it can be concluded that the planned construction of the TEN-T railway connection between the airport on the left side of the Danube River through the city center on the other side of the Danube to the Petržalka region will have varying impacts on the groundwater level regime in the area. Although there will be an increase in the groundwater level regime on the left side of the Danube River, it can be controlled by designing openings in a sealing wall, as proposed by the model. However, no significant impact was observed to the groundwater level regime on the right side of the Danube River in the Petržalka region, and therefore, no additional measures were proposed.

The presented model solution provides valuable information on the potential impacts of the planned construction on the groundwater level regime in the area, and it suggests measures that can be taken to mitigate any adverse effects. The findings of this study are expected to inform decision-making processes on the construction of the TEN-T railway connection and contribute to the development of sustainable infrastructure in the region. Through a thorough analysis of the impacts of the proposed railway line on the groundwater, we developed a solution model that allows for more accurate predictions of the fluctuations in the groundwater levels along the track. This model also provides valuable information about the potential adverse effects and options for mitigation. Specifically, by implementing openings above the railway, we successfully predicted an increase in the level of protection of the surrounding area of the planned railway line by lowering the groundwater level on the western side of the track and increasing it on the eastern side. These findings have significant implications for the decision-making processes and will contribute to the development of sustainable infrastructure. Our study expands knowledge in the field of managing and designing measures to minimize risks and enhance the safety of the railway project.

References

1.　United Nations. *World Urbanization Prospects*; Department of Economic and Social Affairs: New York, NY, USA, 2005.

2.　Pokrajac, D.; Howard, K. Advanced Simulation and Modeling for Urban Groundwater Management—UGROW. *Environ. Model. Softw.* **2013**, *39*, 41–51. [CrossRef]

3.　Attard, G.; Winiarski, T.; Rossier, Y.; Eisenlohr, L. Review: Impact of Underground Structures on the Flow of Urban Groundwater. *Water* **2017**, *9*, 135. [CrossRef]

4.　Pujades, E.; López, A.; Carrera, J.; Vázquez-Suñé, E.; Jurado, A. Barrier Effect of Underground Structures on Aquifers. *Eng. Geol.* **2012**, *145–146*, 41–49. [CrossRef]

5.　Attard, G.; Rossier, Y.; Eisenlohr, L. Underground Structures Increasing the Intrinsic Vulnerability of Urban Groundwater: Sensitivity Analysis and Development of an Empirical Law Based on a Groundwater Age Modeling Approach. *J. Hydrol.* **2017**, *552*, 460–473. [CrossRef]

6.　Font-Capo, J.; Pujades, E.; Vàzquez-Suñé, E.; Carrera, J.; Velasco, V.; Montfort, D. Assessment of the Barrier Effect Caused by Underground Constructions on Porous Aquifers with Low Hydraulic Gradient: A Case Study of the Metro Construction in Barcelona, Spain. *Eng. Geol.* **2015**, *196*, 238–250. [CrossRef]

7.　De Caro, M.; Crosta, G.B.; Previati, A. Modeling the Interference of Underground Structures with Groundwater Flow and Remedial Solutions in Milan. *Eng. Geol.* **2020**, *272*, 105652. [CrossRef]

8.　Ricci, G.; Enrione, R.; Eusebio, A.; Crova, R. Numerical Modeling of the Interference between Underground Structures and Aquifers in Urban Environment: The Turin Subway—Line 1. In *Underground Space—The 4th Dimension of Metropolises*; Barták, V., Hrdina, J., Romancov, M., Zlámal, J., Eds.; Taylor & Francis Group: London, UK, 2007; pp. 649–654, ISBN 978-0-415-40807-3.

9.　Shivaei, S.; Hataf, N.; Pirastehfar, K. 3D Numerical Investigation of the Coupled Interaction Behavior between Mechanized Twin Tunnels and Groundwater—A Case Study: Shiraz Metro Line 2. *Tunn. Undergr. Space Technol.* **2020**, *103*, 103458. [CrossRef]

10.　Xue, T.; Xue, X.; Long, S.; Chen, Q.; Lu, S.; Zeng, C. Effect of Pre-Existing Underground Structures on Groundwater Flow and Strata Movement Induced by Dewatering and Excavation. *Water* **2023**, *15*, 814. [CrossRef]

11.　Zhang, C.; Chen, Z.; Yang, X. The Study about the Integrated Planning Theory of Surface and Underground Urban Space. *Procedia Eng.* **2011**, *21*, 16–23. [CrossRef]

12.　Bobylev, N. Mainstreaming Sustainable Development into a City's Master Plan: A Case of Urban Underground Space Use. *Land Use Policy* **2009**, *26*, 1128–1137. [CrossRef]

13.　Kačo, I.; Chomová, V. The Concept of Interconnecting TEN-T Corridors with the Airport and Railway Network in Bratislava. In Slovak: Koncepcia projektu železničného prepojenia koridorov TEN-T s letiskom a železničnou sieťou v Bratislave. *Tunnel* **2009**, *18*, 3–6.

14.　Baroková, D. Impact Assessment of Proposed Underground Railway Line in Bratislava on Groundwater Regime. In Proceedings of the SGEM 2014, GeoConference on Science and Technologies in Geology, Exploration and Mining STEF92 Technology, Sofia, Bulgaria, 17 September 2014; pp. 495–502. [CrossRef]

15.　Available online: https://www.mapsofworld.com/ (accessed on 20 April 2023).

16.　ÚGKK SR. Map Klient ZBGIS—The Basic Base of the Geographic Information System. Available online: https://zbgis.skgeodesy.sk/mkzbgis/sk/zakladna-mapa/toc?pos=48.800000,19.530000,8 (accessed on 12 March 2021).

17.　Šoltész, A.; Baroková, D. Modeling Solution of the Impact of the Planned TEN-T Underground Railway Line on the Groundwater Flow Regime in the Bratislava Region. In Slovak: *Modelové Riešenie Vplyvu Plánovanej Podzemnej Železničnej Trasy TEN-T na Režim Podzemných vôd v Oblasti Bratislavy*; Scientific Report; Faculty of Civil Engineering, STU: Bratislava, Slovakia, 2007; 65p.

18. Dopravoprojekt Bratislava. *Project TEN-T Connection of the TEN-T Railway Corridor with the Airport and Railway Network in Bratislava*; Documentation for Zoning Decision; Dopravoprojekt Bratislava: Bratislava, Slovakia, 2008.

19. Škvarka, J.; Kupka, Š.; Takáčová, M.; Šikula, G. Study of the connection of the TEN-T railway corridor with the airport and the railway network in Bratislava—Section of the railway line Bratislava Predmestie—Bratislava Filiálka—Bratislava Petržalka. In *Slovak: Štúdia Prepojenia Železničného Koridoru TEN-T s Letiskom a Železničnou Sieťou v Bratislave—Úsek Železničnej Trate Bratislava Predmestie—Bratislava Filiálka—Bratislava Petržalka*; Final Report of Hydro-Geological Survey; Ekogeos: Bratislava, Slovakia, 2007; 35p.

20. Hálek, V.; Kratochvíl, S. *Protection of the Bratislava—Petržalka Region*; Final Report; VUT Brno: Brno, Czechia, 1971; 44p.

21. Hydrogeological Maps [Online]. Bratislava: State Geological Institute of Dionýz Štúr. 2008. Available online: http://apl.geology.sk/hydrogeol (accessed on 2 April 2021).

22. Mucha, I.; Rodák, D.; Hlavatý, Z.; Banský, Ľ.; Kučárová, K. Development of ground water regime in the area of the Gabčíkovo Hydroelectric Power Project. *Slovak Geol. Mag.* **1999**, *5*, 151–167.

23. SHMI Bratislava, Hydrological Yearbook of Surface Water. Delivered in Digital Form. Available online: https://www.shmu.sk/File/Hydrologia/Monitoring_PV_PzV/Monitoring_kvantity_PV/PVkvant2020/HR2020.pdf (accessed on 10 February 2021).

24. SHMI Bratislava, Hydrological Yearbook of Ground Water. Delivered in Digital Form. Available online: https://www.shmu.sk/sk/?page=2649 (accessed on 7 February 2021).

25. Říha, J.; Julínek, T.; Duchan, D. Quantification of Groundwater Hazards Related to Fluvial Floods via Groundwater Flow Modeling: A Review. *Water* **2023**, *15*, 1145. [CrossRef]

26. Dulovičová, R.; Velísková, Y.; Schügerl, R. Assesment of Selected Empirical Formulas for Computation of Saturated Hydraulic Conductivity. *Acta Hydrol. Slovaca* **2021**, *22*, 78–87. [CrossRef]

27. Gomboš, M.; Tall, A.; Trpčevská, J.; Kandra, B.; Pavelková, D.; Balejčíková, L. Sedimentation Rate of Soil Microparticles. *Arab. J. Geosci.* **2018**, *11*, 20. [CrossRef]

28. GKÚ Geodetický a kartografický Ústav. Geodetic and Cartografic Institute in Bratislava. Ortofotomosaic SR. Bratislava. 2021. Available online: https://www.geoportal.sk/sk/udaje/ortofotomozaika/ (accessed on 23 February 2021).

29. Royal Haskoning. *Triwaco User's Manual*; Royal Haskoning: Amsterdam, The Netherlands, 2004.

30. Jazayeri, A.; Werner, A.D. Boundary Condition Nomenclature Confusion in Groundwater Flow Modeling. *Groundwater* **2019**, *57*, 664–668. [CrossRef] [PubMed]

31. Turkyilmazoglu, M.; Siddiqui, A.A. The instability onset of generalized isoflux mean flow using Brinkman-Darcy-Bénard model in a fluid saturated porous channel. *Int. J. Therm. Sci.* **2023**, *188*, 108249. [CrossRef]

32. Anderson, M.P.; Woessner, W.W. *Applied Groundwater Modeling: Simulation of Flow and Advective Transport*; Academic Press, Inc.: San Diego, CA, USA, 1992; 381p.

33. Otto, S.A. How to Normalize the RMSE. [Blog Post]. 7 January 2019. Available online: https://www.marinedatascience.co/blog/2019/01/07/normalizing-the-rmse/ (accessed on 14 June 2023).

34. Waterloo Hydrogeologic. Visual MODFLOW Flex 9.0 Help—Calibration Statistics. Available online: https://www.waterloohydrogeologic.com/help/vmod-flex/index.html?vm_calibration_statistics.htm (accessed on 14 June 2023).

35. Zatlakovič, M.; Krčmář, D.; Hodasová, K.; Sracek, O.; Marenčák, Š.; Durdiaková, Ľ.; Bugár, A. The Impact of Groundwater Model Parametrization on Calibration Fit and Prediction Accuracy—Assessment in the Form of a Post-Audit at the SLOVNAFT Oil Refinery Site, in Slovakia. *Water* **2023**, *15*, 839. [CrossRef]

36. Švasta, J.; Malík, P. Priestorové rozloženie priemerných efektívnych zrážok na území Slovenska: Spatial Distribution of Mean Effective Precipitation over Slovakia. *Podzemn. Voda* **2006**, *12*, 65–77. Available online: http://www.sah-podzemnavoda.sk/cms/e107_plugins/content/content.php?content.295 (accessed on 8 February 2021).